

Analysis of recent VLBI catalogs

Sébastien B. Lambert

SYRTE, Observatoire de Paris, PSL Research University, CNRS, Sorbonne Universités, UPMC Univ. Paris 06, LNE
 61 av. de l'Observatoire, 75014 Paris, France
 Phone: +33 1 40 51 22 33
 E-mail: sebastien.lambert@obspm.fr

Published in [IERS Annual Report 2015](#)

1. Data sets

Six catalogs were submitted respectively by the Italian Space Agency (ASI; asi2015a), Geoscience Australia (aus2015c; aus2016a/b), the Federal Agency for Cartography and Geodesy (BKG Leipzig) and Institute of Geodesy and Geoinformation of the University of Bonn (IGGB) (bkg2015a), and the US Naval Observatory (usn2015b). All these catalogs provide right ascension (α) and declination (δ) of extragalactic radio sources, as well as their respective uncertainties, the correlation coefficient between α and δ , and the number of sessions and delays. Note that bkg2014a and usn2015a were produced with the same geodetic VLBI analysis software package SOLVE developed at NASA GSFC. Solutions aus2015c and aus2016a/b were produced with OCCAM.

Table 1 displays the total number of sources of each catalog, as well as the number of ICRF2 sources (out of 3414) and ICRF2 defining sources (out of 295). Some catalogs do not provide values for some defining sources, likely because they do not process some sessions that were present in the session list processed to generate the ICRF2 catalog. We recommend that the analysis centers pay attention to their session list in order to get values for all 295 ICRF2 defining sources. As well, none of the catalogs provide values for all 3414 ICRF2 sources (it was already pointed in the 2014 Annual Report).

The median error reported in Table 1 reveals an error in declination larger than in right ascension by a factor of ~ 1.5 . The error is substantially smaller for SOLVE solutions compared to OCCAM, except the solution asi2015a whose smaller error likely originates in the fact that the solution considered a relatively small number of well observed sources with low positional standard error.

2. Frame orientation

We evaluate the consistency of the submitted catalogs with the ICRF2 by modeling the coordinate difference (in the sense catalog minus ICRF2) by a 6-parameter transformation as used at the IERS ICRS PC in previous comparisons:

$$\begin{aligned} A1 \tan \delta \cos \alpha + A2 \operatorname{tg} \delta \sin \alpha - A3 + DA (\delta - \delta_0) &= \Delta\alpha, \\ -A1 \sin \alpha + A2 \cos \alpha + DD (\delta - \delta_0) + BD &= \Delta\delta, \end{aligned}$$

where $A1, A2, A3$ are rotation angles around the X, Y, and Z axes of the celestial reference frame, respectively, DA and DD represent linear variations with the declination (which origin δ_0 can be arbitrarily chosen but was set to zero in this study), BD is a bias in declination, and $\Delta\alpha$ and $\Delta\delta$ are coordinate differences between the studied and the ICRF2 catalogs. The 6 parameters were fitted by weighted least squares to the coordinate difference of the defining sources (upper part of Table 2) and ICRF2 sources (lower part of Table 2) found in the catalog. The standard deviation of the offsets to ICRF2 after removal of the systematics of Table 2 is reported in Table 3 together with the median offset.

The three Australian solutions show non statistically significant rotations and deformations with respect to the ICRF2. Significant misorientation around $A2$ larger than 10 mas (4 sigmas) are found for other catalogs. The largest deviation from ICRF2 axes is observed for the bias in declination. Values of BD are significantly larger than the ICRF2 axis stability of 10 mas measured at the time of the ICRF2 release in 2009 (Fey et al. 2015). This fact may indicate some systematics in source declinations with respect to solutions of the previous years and

may have to be considered in parallel to the zonal declination error raised in the 2012—2015 ICRF3 WG documentation (e.g., Jacobs et al. 2014). Note that this particular point should be addressed rigorously in the framework of the 2016—2018 ICRF3 WG.

3. Zonal errors

Figure 1 displays the offset to ICRF2 (in the sense catalog minus ICRF2) averaged over declination bins of 5 degrees. All solutions but Australian ones exhibit declination errors offset to the negative part of the plot, that may reflect the large values of BD found in the coordinate difference to ICRF2. However, no pronounced dependence in declination shows up for any solution.

4. Standard error and noise

Figure 2 illustrates how the overall formal error, defined as the square root of $\sigma_{\alpha\cos\delta}^2 + \sigma_{\delta}^2 + c\sigma_{\alpha\cos\delta}\sigma_{\alpha\delta}$ where σ is the formal error listed in the catalogs and c is the correlation coefficient between estimates of α and δ as provided in the catalogs, varies with the number N of observations. The circled dots represent defining sources. The figure for aus2016b clearly shows that the defining sources have underestimated formal errors likely due to an overconstrained solution. (As stated in the technical document delivered with the catalog, a strong no-net rotation condition imposed to these sources. Similar fact was pointed for solution aus2015a in the 2014 IERS Annual Report.) The formal error of the same sources in solution aus2015c and aus2016a, in which the no-net rotation condition is less severe, appears to be at a level comparable to other sources.

Figure 2 also shows how the error on delays is propagated to the estimated source coordinates. For white noise measurements, the formal error on source coordinates is expected to decrease as $N^{-0.5}$. The figure reveals that this regime exists for N between ~ 100 and ~ 10000 . For N lower than a hundred observations (e.g., VCS sources or sources observed in only one session) the formal error varies as N^{-1} . Beyond 10000 observations, the formal error generally tends towards a limit lower than ~ 10 mas. Such a deviation is visible for all catalogs but the Australian ones for which the formal error seems to continue to decrease more closely (but not exactly) to $N^{-0.5}$. The deviation for large N observed for all other catalogs is likely the signature of non-Gaussian correlated errors: as N increases, thermal baseline-dependent error tends to zero and the station-dependent error arising from time- and space-correlated parameters becomes dominant (see, e.g., Gipson 2006 or Romero-Wolf et al. 2012; see also Lambert 2014).

A last test was performed to assess the consistency between the formal errors and the offset to ICRF2. This test was motivated by the consideration that, although the ICRF2 is not the “truth”, it nevertheless provides accurate values of well-observed sources. As a consequence, for most of the sources, the addition of new observations after 2009 should not perturb significantly the estimated position but only improve the formal error. Figure 3 displays the scatter around the ICRF2 position computed for bins of increasing formal error. For a white noise, one should get values close to the first diagonal (i.e., the formal error fully explains the offset to ICRF2). For formal errors lower than 0.1 mas, one sees that the scatter is over the diagonal, indicating a possible underestimation of the formal errors. To quantify this scale factor, one can estimate it together with an error floor so that a realistic error E_r (i.e., that explains the observed offset to ICRF2) is given by

$$E_r = ((E s)^2 + f^2)^{-0.5}$$

where E is the error, s a scale factor and f a noise floor. Values of s and f estimated over sources whose offset to ICRF2 is smaller than 1 mas are reported in Table 4. Uncertainties are ~ 0.01 mas on s and ~ 0.01 on f . SOLVE solutions tend to have scale factors larger than unity while OCCAM catalogs have scale factors smaller than 1. Note that the noise floor does not represent the catalog internal error since one considers the offset to ICRF2: the quantity f therefore contains the internal noise of the ICRF2. The global noise lies between 0.05 and 0.12 mas. If one assumes 0.04 mas for the ICRF2 internal noise (Fey et al. 2015), it means that the analyzed catalog internal noises are larger by a factor between 1 and 3.

5. Conclusions and recommendations

The above results lead to some recommendations for analysis centers who plan new submissions in the future. First, it is recommended to include all ICRF2 sessions in the processed session list, in order to get values of, at least, all 3414 ICRF2 sources. Second, analysis centers should focus on understanding several points: (i) the significant systematics in orientation (~ 0.05 mas) showing up in Table 2, (ii) the zonal errors appearing in Fig. 1 for some solutions, and (iii) the non-Gaussian errors dominating for large number of observations raised by

Fig. 3. About the latter item, one should understand particularly why the OCCAM solutions decreases differently than SOLVE catalogs for larger numbers of delays. In the future, the correction of this defect should be achieved by better modeling and parameterization of clock and troposphere correlated errors, consistently in all VLBI analysis softwares.

Table 1. Number of sources by categories and median error. Unit is mas. Values for right ascension are corrected from the cosine of the declination.

	----- No. Sources -----			-- Median Error --	
	Total	ICRF2	Def	RA	Dec
asi2015a	944	936	294	37.3	41.2
aus2015c	3683	3235	295	1276.5	1780.0
aus2016a	3900	3282	295	526.5	728.0
aus2016b	3917	3288	295	520.5	700.0
bkg2015a	3398	3112	294	284.6	430.2
usn2015b	4110	3316	287	231.0	333.7

Table 2. Rotation parameters with respect to ICRF2. A1, A2, A3 and BD are in mas. DA and DD are in mas per degree.

	A1	A2	A3	DA	DD	BD
----- Defining sources -----						
asi2015a	-2.3	16.4	-13.1	0.2	1.0	-68.5
+-	3.6	3.6	3.3	0.1	0.1	3.5
aus2015c	-9.5	2.9	2.2	-0.0	0.2	3.0
+-	3.0	3.0	2.9	0.1	0.1	2.9
aus2016a	-6.3	2.1	4.5	-0.0	-0.0	4.2
+-	3.4	3.4	3.2	0.1	0.1	3.3
aus2016b	-4.6	-0.3	4.8	0.1	-0.1	4.8
+-	3.0	3.0	2.8	0.1	0.1	2.9
bkg2015a	-9.3	12.3	-9.1	0.2	1.1	-64.2
+-	4.3	4.3	3.8	0.1	0.1	4.2
usn2015b	-7.2	16.3	-0.4	0.2	0.9	-53.2
+-	3.8	3.8	3.3	0.1	0.1	3.6
----- All common sources -----						
asi2015a	2.5	18.9	-14.1	0.2	1.2	-70.6
+-	2.8	2.8	2.6	0.1	0.1	2.6
aus2015c	-4.4	2.2	-3.9	-0.1	0.3	0.6
+-	1.2	1.2	1.2	0.0	0.0	1.1
aus2016a	-1.8	1.3	-3.3	-0.2	0.1	1.2
+-	1.2	1.2	1.1	0.0	0.0	1.1
aus2016b	-0.5	0.1	-0.2	-0.0	0.0	0.2
+-	0.2	0.2	0.2	0.0	0.0	0.2
bkg2015a	-4.1	14.7	-10.9	0.1	1.3	-66.2
+-	1.5	1.5	1.4	0.1	0.0	1.4
usn2015b	-2.8	20.4	-7.1	-0.0	1.1	-57.2
+-	1.4	1.4	1.3	0.0	0.0	1.3

Table 3. Statistics after removal of systematics given in Tables 2. Unit is mas. Values for right ascension are corrected from the cosine of the declination.

	---- Standard Deviation ----				----- Median Offset -----			
	- Defining -		---- All ----		- Defining -		---- All ----	
	RA	Dec	RA	Dec	RA	Dec	RA	Dec
asi2015a	55.5	64.8	141.6	323.6	49.7	61.4	50.3	61.4
aus2015c	53.6	48.5	128.4	161.2	247.5	488.0	269.2	450.6
aus2016a	51.9	43.9	139.4	173.0	247.9	442.3	261.7	438.3
aus2016b	7.8	5.5	33.2	39.3	242.4	455.6	246.6	414.8
bkg2015a	53.7	61.8	362.7	364.1	118.1	222.5	121.5	209.2
usn2015b	60.0	65.4	565.1	863.2	126.5	238.4	134.7	230.4

Table 4. Noise floor and scale factor estimated for sources with offset lower than 1 mas. Unit is uas. Values for right ascension are corrected from the cosine of the declination.

	-- Floor --		-- Scale --	
	RA	Dec	RA	Dec
asi2015a	42.7	55.6	3.65	3.07
aus2015c	46.7	40.5	0.60	0.60
aus2016a	48.3	43.6	1.14	1.11
aus2016b	7.3	7.7	1.17	1.12
bkg2015a	50.7	66.4	1.34	1.18
usn2015b	57.6	71.2	1.64	1.54

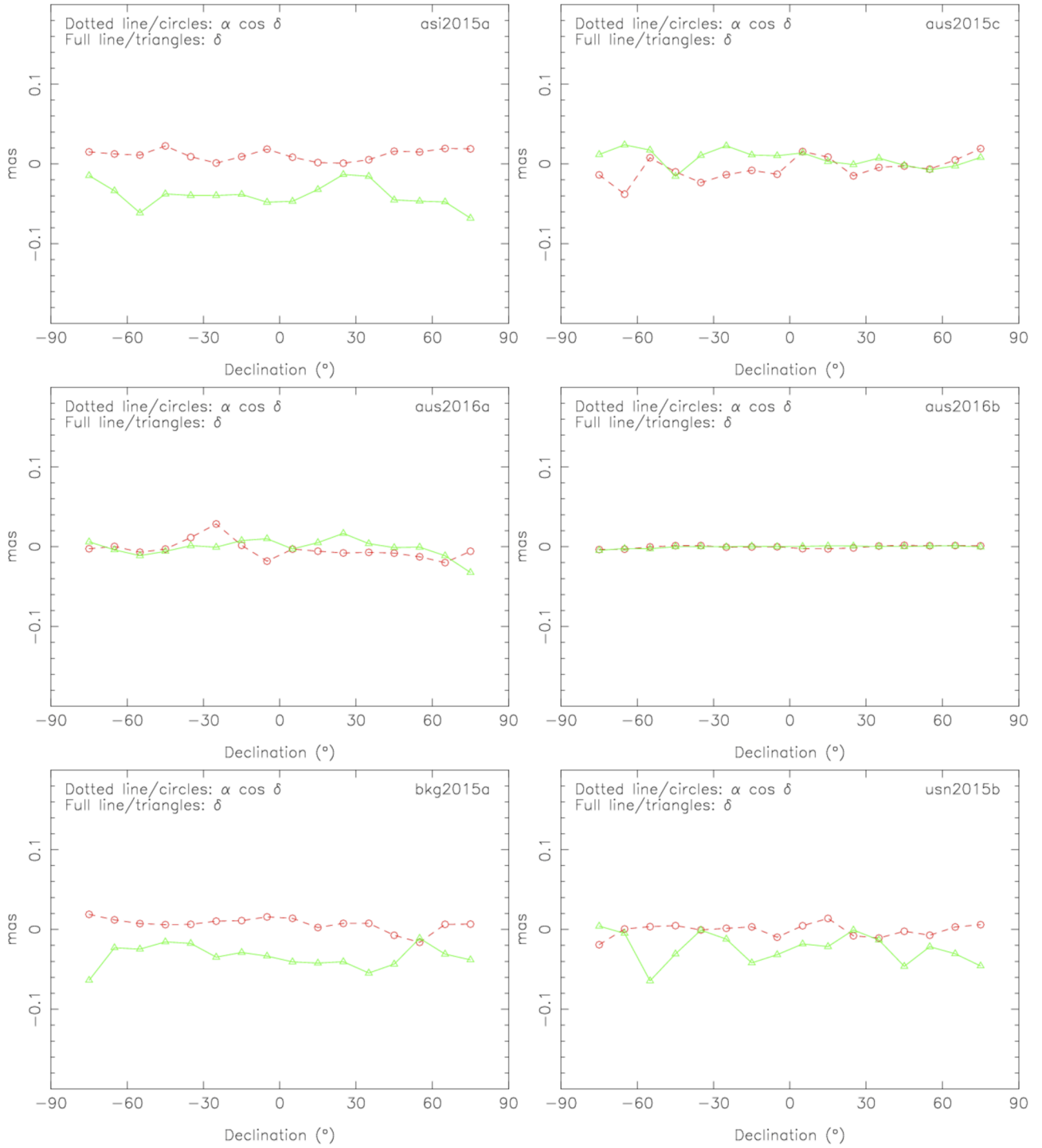


Fig. 1. Offset to ICRF2 for right ascension (dotted line with circles) and declination (full line with triangles) by bins of declination of 5 degrees.

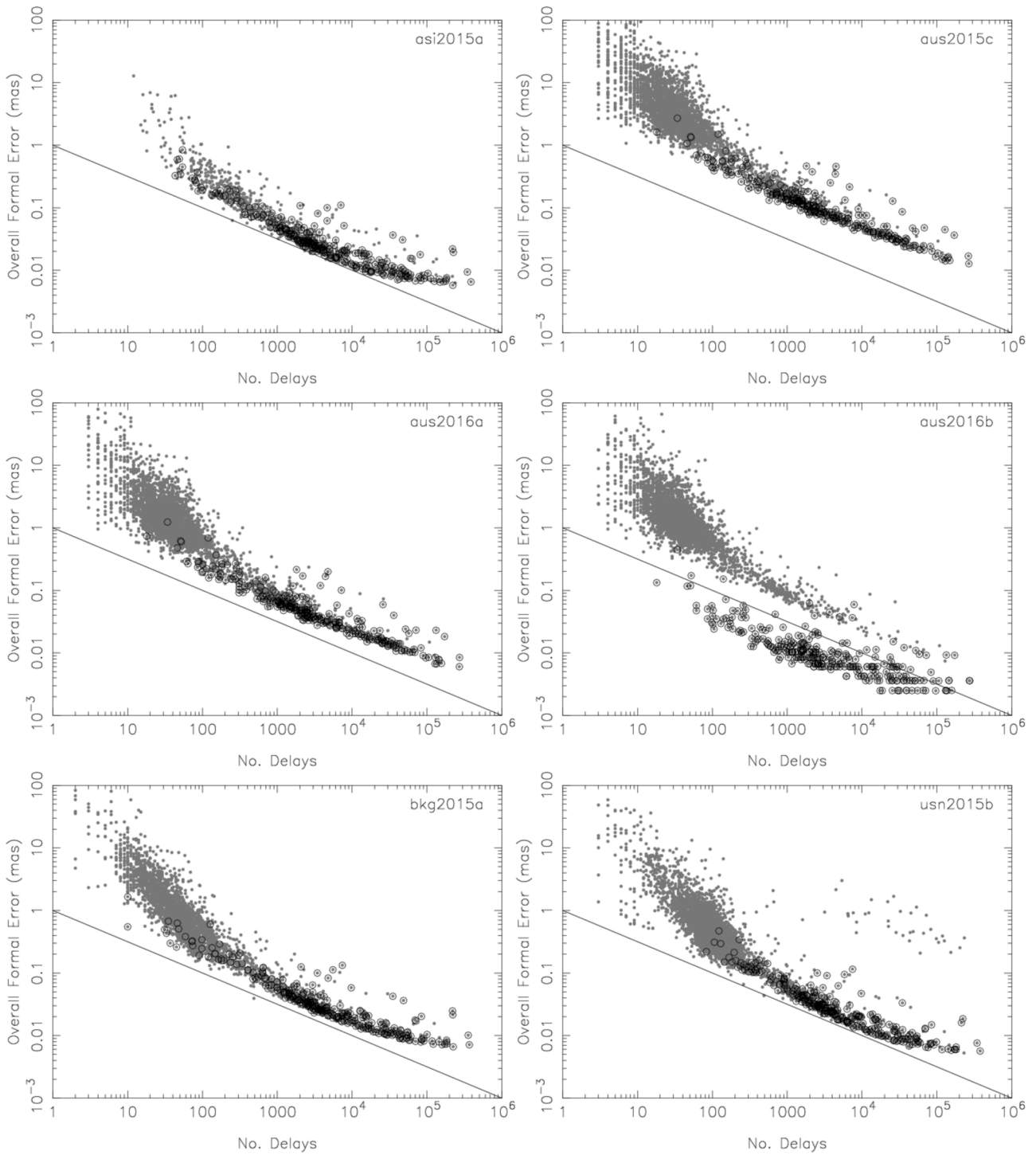


Fig. 2. Overall formal error as a function of the number of observations. The circled dots represent defining sources. The solid line indicates a decrease as $N^{-1/2}$ where N is the number of delays.

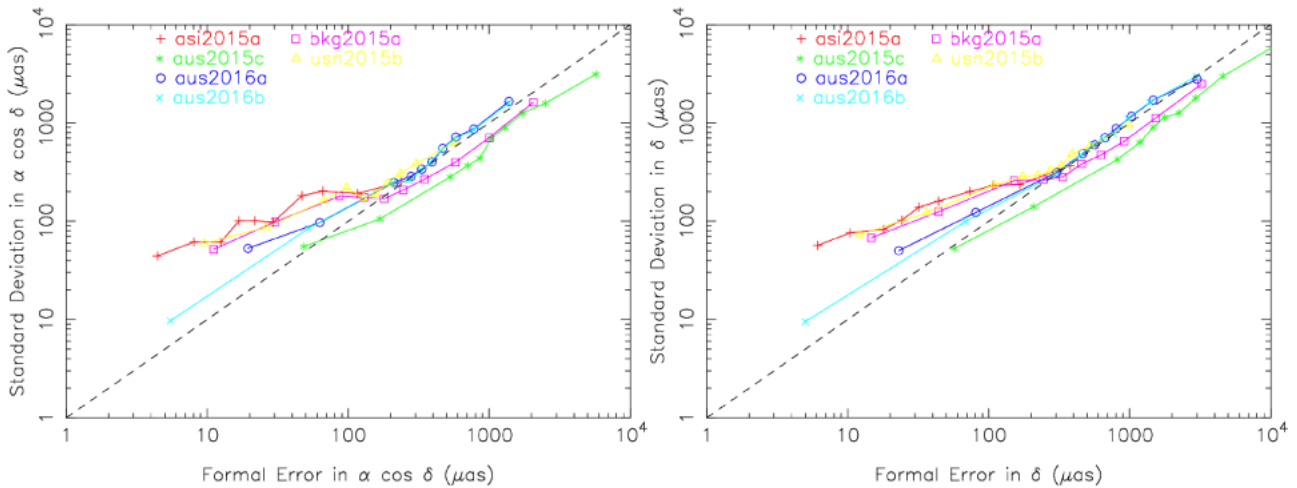


Fig. 3. Scatter of the offset to ICRF2 versus the formal error.

6. References

Fey, A. L., Gordon, D., Jacobs, C. S., Ma, C., Gaume, R. A., Arias, E. F., Bianco, G., Boboltz, D. A., Böckmann, S., Böhm, J., Bolotin, S., Charlot, P., Collioud, A., Engelhardt, G., Gipson, J., Gontier, A.-M., Heinkelmann, R., Kurdubov, S., Lambert, S., Lytvyn, S., MacMillan, D. S., Malkin, Z., Nothnagel, A., Ojha, R., Skurikhina, E., Sokolova, J., Souchay, J., Sovers, O. J., Tesmer, V., Titov, O., Wang, G., & Zharov, V. 2015, The second realisation of the International Celestial Reference Frame by very long baseline interferometry, *Astron. J.*, 150, 58

Gipson, J. M. 2006, in *International VLBI Service for Geodesy and Astrometry (IVS) 2006 General Meeting Proceedings*, NASA/CP-2006-214140, eds. D. Behrend, & K. D. Baver, 286

Jacobs, C. S., Arias, E. F., Boboltz, D., Boehm, J., Bolotin, S., Bourda, G., Charlot, P., de Witt, A., Fey, A. L., Gaume, R. A., Gordon, D., Heinkelmann, R., Lambert, S. B., Ma, C., Malkin, Z., Nothnagel, A., Seitz, M., Skurikhina, E., Souchay, J., Titov, O. A. 2014, In: *Proceedings of the Journées 2013 "Systèmes de référence spatio-temporels": Scientific developments from highly accurate space-time reference systems*, Observatoire de Paris, 16-18 September 2013, Edited by Nicole Capitaine, ISBN 978-2-901057-69-7, 51

Lambert, S. 2014, Comparison of VLBI radio source catalogs, *Astron. Astrophys.*, 570, 108

Romero-Wolf, A., Jacobs, C. S., & Ratcliff, J. T. 2012, in *International VLBI Service for Geodesy and Astrometry (IVS) 2012 General Meeting Proceedings*, NASA/CP-2012-217504, eds. D. Behrend, & K. D. Baver, 231